

Reconstruction of Hadronization Stage in Pb+Pb Collisions at 158A GeV/c

S.V. Akkelin¹, P. Braun-Munzinger², and Yu.M. Sinyukov¹

Recent data on hadron multiplicities in central Pb+Pb collisions at 158A GeV/c at mid-rapidity are analyzed within the concept of chemical freeze-out. A non-uniformity of the baryon chemical potential along the beam axis is taken into account. An approximate analytical solution of the hydrodynamic equations for a chemically frozen Boltzmann-like gas is found. The Cauchy conditions for hydrodynamic evolution of the hadron resonance gas are fixed at the thermal freeze-out hypersurface from analysis of one-particle momentum spectra and Bose-Einstein (HBT) correlations. The proper time of chemical freeze-out and physical conditions at the hadronization stage, such as energy density and averaged transverse velocity, are found.

¹ *Bogolyubov Institute for Theoretical Physics, Kiev 03143, Metrologicheskaya 14b, Ukraine.*

² *Gesellschaft für Schwerionenforschung, D-64291 Darmstadt, Germany.*

PACS: 24.10.Nz, 24.10.Pa, 25.75.-q, 25.75.Gz, 25.75.Ld.

Keywords: relativistic heavy ion collisions, hadronization, chemical freeze-out, kinetic (thermal) freeze-out, hydrodynamic evolution, hadron resonance gas, quark-gluon plasma, inclusive spectra, HBT correlations.

Corresponding author: Yu.M.Sinyukov, Bogolyubov Institute for Theoretical Physics, Kiev 03143, Metrologicheskaya 14b, Ukraine. E-mail: sinyukov@gluk.org, tel. +380-44-2273189, tel./fax: 380-44-4339492

I. INTRODUCTION

Systems which are created in ultra-relativistic A+A collisions at SPS and RHIC are initially very dense and display collective behavior. The quasi-macroscopic nature of those systems allows to study new states of matter at the phase boundary between a hadron gas (HG) and the quark-gluon plasma (QGP). Among the different methods to study it, an important role belongs to precise measurement of hadronic observables. One- and multi-particle hadron spectra, however, do not carry direct information about the phase transition since one should expect strong interactions in the hadron resonance gas after hadronization. Usually, different theoretical approaches are used to diagnose the matter properties at the transition point. A rather fruitful concept is that of chemical freeze-out. It implies, first, that the initial hadronic state is in chemical equilibrium [1,2]. Second, the chemical concentrations of HG do not change during the evolution. The latter assumption is justified by the observation that the rate of expansion in HG is larger than the rate of inelastic reactions and less than that of elastic collisions [3]. It gives the possibility to use the approach of local thermal equilibrium and hydrodynamic expansion of HG at approximately frozen chemical composition. The initial conditions for the hadronic stage of the collective expansion are determined by matter evolution in the pre-hadronic phase and also by particle interactions and hadronization conditions.

If chemical freeze-out takes place, it is defined by a temperature and chemical potentials conjugated to conserved quantum numbers. To extract those thermodynamic parameters from total particle number ratios one has to assume uniform temperature, baryon and strangeness chemical potentials as well as a unique hadronization hypersurface $\sigma^{ch}(x)$ for all particles. The result is a common effective volume for all hadron species, that completely absorbs effects of flow and a form of the hypersurface and approximately cancels in a description of particle ratios [4].

In detail, the situation may be somewhat more complicated. While baryon stopping seems to be fairly complete at AGS energies [5] (see also Ref. [6] where possible deviations from the full stopping are analyzed quantitatively), there are clear indications for an onset of transparency at top SPS energy from the observed fairly flat rapidity distribution of pions in Pb+Pb central collisions [7,8] and, in particular, from the difference in rapidity distributions between protons and antiprotons, which cannot be explained by longitudinal flow developing after full stopping. As a consequence, one could expect particle number ratios taken in mid-rapidity, especially involving nucleons, to differ somewhat from those integrated over 4π . On the other hand, a consistent hydrodynamic analysis then must be based on an analysis of data in a narrow mid-rapidity region, which is done in this paper. We also note that, in a boost-invariant scenario as observed at RHIC, chemical freeze-out conditions are the same for any individual rapidity slices taken within a wide enough rapidity interval.

The object of this paper is to reconstruct the hadronization stage within the hydrodynamic approach. We assume that hadronic matter at that stage has locally a maximal entropy. Effects of hadron-hadron interaction (excluded volumes [9], mean field [10]) as well as specific conditions of hadronization (e.g., possible conservation of number of quarks during the hadronization [11]) are rather complicated and model dependent. So it is naturally to use minimal number of parameters and take all that into account in the simplest way, i.e., as a unique factor changing the particle

numbers. In other words, we describe the system at the stage of hadronization as a mixture of ideal gases with additional common chemical potential μ_{ch} . Afterwards the system expands hydrodynamically with frozen chemical composition, cools down and finally decays at some thermal freeze-out hypersurface $\sigma^{th}(x)$ which could be different for different particle species [12]. Then long-lived particles stream freely into detectors, resonances decay and also contribute to spectra of observed particles. We reconstruct a state of the system at the earlier hadronization stage, find energy and particle number densities and also estimate roughly the effects of interaction at the hadronization stage using an approach described in the following.

From the analysis of slopes of transverse momentum spectra and of interferometry radii for different particle species one can restore the space-time extensions, collective flow parameters and temperature at the thermal freeze-out stage, when the thermal system decouples and particle momentum distributions change no longer. The method of joint analysis of the spectra and correlations was used in Refs. [4,13–15] to reconstruct the thermal freeze-out stage. Note that, to evaluate the detailed behavior of the (pion) spectrum in the whole transverse momentum region, one needs in detail knowledge of the unobserved resonance yields. They can be estimated from the temperature and baryochemical potential at chemical freeze-out. An attempt to determine the resonance yields in that way was undertaken in Ref. [14]. There however, a trajectory assuming isentropic expansion in full chemical equilibrium was employed following Ref. [12], in contradistinction to the assumption of chemical freeze-out. In this paper we make a new analysis of the thermal freeze-out stage within the hydrodynamic approach for lead-lead collisions based on recent experimental data on one particle spectra and HBT correlations for *different* hadron species. We estimate the basic parameters at thermal freeze-out from an analysis of the slopes of particle spectra and of the correlation functions at regions of high enough transverse momentum to minimize the influence of resonance decays. We use also the previous results from Refs. [14,15] to determine the influence of uncertainties in reconstruction of the thermal freeze-out stage on the reconstruction of the hadronic gas parameters at chemical freeze-out.

Recent evidence [1,2,16] support strongly the early interpretation [17] that chemical freeze-out at SPS and higher energies takes place at or near to the phase boundary (see also the discussion in [18]). We employ a similar approach here with emphasis on the analysis of particle ratios near mid-rapidity. To complete the reconstruction of the hadronization stage and find its space-time extension, we solve the hydrodynamic equations with the Cauchy conditions that are found at thermal freeze-out, and consider the solution backwards in time until the chemical freeze-out temperature is reached. The method leads to unique results due to the scale invariance of the hydrodynamic equations for a mixture of ideal Boltzmann gases with reference to scale-transformations of pressure and densities of energy and particles at a fixed temperature. For such a system the variation of initial densities by a unique factor results in the same scale transformation of the solutions. Therefore, the temperature as function of time does not depend on the common chemical potential, which defines absolute values of densities: the temperature depends only on concentrations of different particles species. The latter do not change during the hydrodynamic evolution and are determined by the baryonic and strangeness chemical potentials and temperature just after hadronization. Finally, from reconstructed space-time extension of the chemical freeze-out and a particle numbers in mid-rapidity we determine the densities at hadronization and the common chemical potential.

An alternative way to determine hadron gas parameters is used in Ref. [12]. There, a hydrodynamic approach is followed from the initial condition of an equilibrated QGP through the phase transition and hadronization. Subsequent to hadronization the system is assumed, in fact, to evolve as a mixture of mutually non-interacting gases with fixed chemical composition. In the present approach we, instead, solve the hydrodynamic equations for a complete system under the explicit condition of particle numbers conservation. The distinctive feature of our method is the analysis backwards in time.

In Sec. II we discuss the possibility to extract the thermodynamic parameters at chemical freeze-out from the particle number ratios when those parameters are non-uniformly distributed in rapidity. In Sec. III we consider the particle number ratios in a hydrodynamic approach to A+A collisions. The optimization procedure is applied to fit recent experimental data for Pb+Pb (CERN, SPS) collisions and find the temperature, baryonic and strangeness chemical potentials at chemical freeze-out. In Sec. IV we analyze the property of hydrodynamic expansion in a central slice of space-time rapidity for a chemically frozen mixture of ideal Boltzmann gases. Approximate hydrodynamic solutions for non-relativistic transverse flows are found. In Sec.V the Cauchy conditions at thermal freeze-out, such as proper time, temperature and transverse velocities are defined from the analysis of spectra and Bose-Einstein correlations. In Sec.VI the corresponding “inverse in time” hydrodynamic solution is analyzed and the space-time characteristics of the matter at the hadronization stage are reconstructed. The later are applied to restore the energy and particle number densities at that stage. The conclusions and a discussion of the results are presented in Sec.VII.

II. THE PARTICLE NUMBERS AT MID-RAPIDITY FOR EXPANDING HG

We assume that just after hadronization, the system can be described at some hypersurface $\sigma^{ch}(x)$ as a locally and chemically equilibrated expanding hadron resonance gas. The effects of interaction and possible peculiarities of the hadronization process are taken into account by a common factor changing particle numbers in the ideal gas; the factor is associated with an additional common chemical potential μ_{ch} . In concrete evaluations, as was performed by many authors, instead of considering a finite chemical and thermal freeze-out hypersurfaces $\sigma(x)$ in Minkovsky space, we use the common profile factor $\rho(x)$ at proper time $\tau(r) \approx const$ to guarantee the finiteness of the system (see the discussion on the validity of such an approximation in [13]). Then the total multiplicity of a particle species i at chemical freeze-out is calculated by

$$N_i = \int \frac{d^3p}{p^0} d\sigma_\mu^{ch}(x) p^\mu f\left(\frac{p_\mu u^\mu(x)}{T_{ch}(x)}, \frac{\mu_{i,ch}(x)}{T_{ch}(x)}\right) \rho(x), \quad (1)$$

where $f(p_\mu u^\mu(x)/T_{ch}(x), \mu_{i,ch}(x)/T_{ch}(x))$ is the Bose-Einstein or Fermi-Dirac distribution function in our approach, and $\mu_{i,ch} = B_i \mu_B + S_i \mu_S + \mu_{ch}$. The additional chemical potential μ_{ch} is unique for all particles species. The effect of isotopic chemical potential has been investigated in [2] and found to be small. It is neglected in this paper. Taking into account the invariance of the distribution function under Lorentz transformation, one can carry out integrations over momentum variables and finally get

$$N_i = \int d\sigma_\mu^{ch}(x) u^\mu(x) n_i^{ch}(x), \quad n_i^{ch}(x) = \bar{n}_i^{ch}(x) \rho(x) \quad (2)$$

where in Boltzmann approximation for the distribution function the thermodynamic densities $\bar{n}_i^{ch}(x)$ have the form

$$\bar{n}_i^{ch}(x) = \frac{(2J_i + 1)}{2\pi^2} T_{ch}(x) m_i^2 \exp(\mu_{i,ch}(x)/T_{ch}(x)) K_2(m_i/T_{ch}(x)), \quad (3)$$

and $K_n(u) = \frac{1}{2} \int_{-\infty}^{+\infty} dz \exp[-u \cosh z + nz]$, with $\text{Re } u > 0$, is the modified Bessel function of order n ($n = 0, 1, \dots$). One can rewrite (2) in the form

$$N_i = \langle \bar{n}_i^{ch} \rangle V^{ch} \quad (4)$$

where the volume V^{ch} of system is expressed through the integral of the hydrodynamic 4-velocity $u^\mu(x)$ and the profile factor $\rho(x)$ over the hypersurface σ^{ch} :

$$V^{ch} = \int d\sigma_\mu^{ch}(x) u^\mu(x) \rho(x). \quad (5)$$

We further define the density averaged over the chemical freeze-out hypersurface by

$$\langle \bar{n}_i^{ch} \rangle = \frac{\int d\sigma_\mu^{ch} u^\mu(x) \bar{n}_i^{ch}(x) \rho(x)}{\int d\sigma_\mu^{ch} u^\mu(x) \rho(x)}. \quad (6)$$

If temperature and chemical potentials are uniform over the chemical freeze-out hypersurface, then $\langle \bar{n}_i^{ch} \rangle = \bar{n}_i^{ch}(T_{ch}, \mu_{i,ch})$ and the standard analysis of particle number ratios in 4π geometry can be performed to find the temperature and chemical potentials. However, if T and μ are not uniformly distributed over the hydrodynamic tube at the hypersurface σ^{ch} , then the similar analysis implying the substitution $\langle \bar{n}_i \rangle \rightarrow \bar{n}_i^{ch}(\langle T_{ch} \rangle, \langle \mu_{i,ch} \rangle)$ with some average temperature and chemical potentials, could result in significant deviations for the values one is interested in [19]. To reduce the corresponding uncertainties, the analysis of particle ratios in a narrow rapidity interval near mid-rapidity should be used as we will discuss below.

To analyze non-uniformly distributed systems, let us start from the well known observation [20] that, at the latest stage of a hydrodynamic evolution, the longitudinal velocity distribution corresponds to the asymptotic quasi-inertial regime, $v_L = z/t$. This property, which is the ansatz in the Bjorken model [21] for each moment of time, is realized at the freeze-out stage even in the Landau model of complete stopping [20].¹ Consequently, we assume in the following

¹The asymptotic quasi-inertial property one can see also in the analytic solutions for elliptic flow in non-relativistic approximation [22].

the boost-invariance for longitudinal hydrodynamic velocities at the last (hadronic) stage of the evolution, $v_L = z/t$. This then allows us to parameterize t and z at σ by the form: $t = \tau(r, \eta) \cosh(\eta)$, $z = \tau(r, \eta) \sinh(\eta)$, where r is absolute value of the transverse coordinate \mathbf{r} and η is the longitudinal fluid rapidity, $\eta = \tanh^{-1} v_L$. The parameter $\tau(r, \eta)$ generalizes the Bjorken proper time parameter τ . Taking into account also a transverse velocity component ($v(r, \tau)$ in the longitudinally co-moving system, LCMS), we obtain for the 4-velocity

$$u^\mu(r, \eta) = \gamma (\cosh \eta, v \cos \phi, v \sin \phi, \sinh \eta), \quad (7)$$

where $\gamma = (1 - v^2)^{-1/2}$. The element of the hypersurface $\sigma(x)$ takes the form

$$d\sigma_\mu = \tau(r, \eta) d\eta dr_x dr_y \left(\frac{1}{\tau} \frac{d\tau}{d\eta} \sinh \eta + \cosh \eta, -\frac{d\tau}{dr_x}, -\frac{d\tau}{dr_y}, -\frac{1}{\tau} \frac{d\tau}{d\eta} \cosh \eta - \sinh \eta \right). \quad (8)$$

Let us, first, introduce for an expanding HG the effective volume V_{eff} attributed to one unit of rapidity. To determine V_{eff} one can write the particle number distribution differential in fluid rapidity η for particle of species "i" at chemical freeze-out:

$$\frac{dN_i}{d\eta} = \int \frac{d^3p}{p^0} \frac{d\sigma_\mu^{ch}}{d\eta} p^\mu f \left(\frac{p_\mu u^\mu(r, \eta)}{T_{ch}(\eta)}, \frac{\mu_{i, ch}(\eta)}{T_{ch}(\eta)} \right) \rho(r, \eta). \quad (9)$$

Here we assume that the chemical potentials as well as the temperature are constants in transverse direction across the freeze-out hypersurface. Taking into account the invariance of the distribution function under Lorentz transformation, one can carry out integrations over momentum variables and finally gets

$$\frac{dN_i}{d\eta} = V_{eff}^{ch}(\eta) \bar{n}_i^{ch}(\eta) \quad (10)$$

and

$$V_{eff}^{ch}(\eta) = \int \frac{d\sigma_\mu^{ch}}{d\eta} u^\mu(r, \eta) \rho(r, \eta). \quad (11)$$

The particle number distribution over momentum rapidity y is

$$\frac{dN_i}{dy} = \int \frac{d^3p}{p^0 dy} d\sigma_\mu^{ch} p^\mu f \left(\frac{p_\mu u^\mu(r, \eta)}{T_{ch}(\eta)}, \frac{\mu_{i, ch}(\eta)}{T_{ch}(\eta)} \right) \rho(r, \eta). \quad (12)$$

One can rewrite Eq.(12) in the form

$$\frac{dN_i}{dy} = \frac{dN_i}{d\eta} \Big|_{\eta=y} (1 + \delta_i(y)) = V_{eff}^{ch}(y) (1 + \delta_i(y)) \bar{n}_i^{ch}(y) \quad (13)$$

where

$$\delta_i(y) = \frac{\frac{dN_i}{dy} - \frac{dN_i}{d\eta} \Big|_{\eta=y}}{\frac{dN_i}{d\eta} \Big|_{\eta=y}} \quad (14)$$

From Eq.(13), one can conclude that, for a nonuniform distribution of thermodynamic parameters along the beam axis, the analysis of particle number ratios at mid-rapidity, $y \approx 0$ can be based on ratios \bar{n}_i/\bar{n}_j if correction factors $\delta_i(0)$ are small. One can include corresponding corrections in the non-unique "effective volume" $V_{eff, i}^{ch} = V_{eff}^{ch} (1 + \delta_i)$ which is different for different particle species.

Let us estimate the correction factors. The saddle-point approximation to the integrals over fluid rapidity η in (12) can be applied when the parameter $m_i/T(\eta) \gg 1$ at the saddle point $\eta \approx y$. Then, at mid-rapidity, the area around $\eta = y = 0$ gives the main contribution to the integral over η in (12) and one can expand the slowly varying functions into a Taylor series around the saddle-point $\eta = 0$. We neglect a variation of $T(\eta)$ in space rapidity η in comparison with the variation of $\mu_i^{ch}(\eta)$, assuming that all non-uniformity originated from incomplete baryonic stopping. This implies an increase of the baryonic chemical potential with the absolute value of rapidity. Assuming that the transverse expansion is non-relativistic, with a freeze-out that occurs at approximately equal proper time τ , and that the profile $\rho(x)$ can be factorized, $\rho(x) = \rho_T(r) \rho_L(\eta)$, we estimate the correction factor at mid-rapidity:

$$\delta_i \approx \frac{1}{2} \frac{(\rho_L \exp(\mu_{i,ch}/T_{ch})\tau_{ch})''|_{\eta=0} T_{ch}}{\rho_L(0) \exp(\mu_{i,ch}/T_{ch})\tau_{ch} m_i} \quad (15)$$

All thermodynamic parameters here are taken at mid-rapidity. One can see that the factor δ_i is rather small for baryons, because the ratio T_{ch}/m_i is small, as well as it is small for pions, because their baryonic number are equal to zero. Therefore, as follows from Eq.(13) for $\delta_i \ll 1$ the analysis of particle number ratios at a narrow mid-rapidity interval can be based on ratios $\bar{n}_i^{ch}/\bar{n}_j^{ch}$ [4]. These values are the same as for Boltzmann gas in a static volume.

It is worth to note that the second derivative in formula (15) is positive for incomplete baryonic stopping and, so, $\delta_i > 0$. As we will discuss later, the consequences of it are non-trivial and rather important for pion production via decay of baryonic resonances after the thermal freeze-out occurs. Note that the hadron production at thermal freeze-out, in fact, can be described by the equations of this section with the substitutions $ch \rightarrow th$ and, taking into account the absence of chemical equilibrium at thermal freeze-out: $\mu_{i,th}$, cannot be expressed via two common independent parameters and the quantum numbers of particle i in the way as it was done for $\mu_{i,ch}$.

III. THE ANALYSIS OF PARTICLE NUMBER RATIOS

In ultrarelativistic A+A collisions a hadron resonance gas is assumed to appear due to the hadronization process. Subsequent, it expands and reaches the final stage of the evolution - the thermal freeze-out. According to the hypotheses of chemical freeze-out, the total number of each particle species is preserved during the evolution. After the hydrodynamic tube decays and produces final particles, one has to take into account also particles that come from resonance decays. In our calculations the resonance mass spectrum extends over all mesons and baryons with masses below 2 GeV. Decay cascades are also included in the analysis. The value of the strangeness chemical potential μ_S is fixed by baryonic chemical potential and temperature from the condition of local strangeness conservation. We optimize the particle number ratios at mid-rapidity, using the corresponding values for Pb + Pb collisions at 158A GeV/c from WA97 (Table 1) and NA49 (Table 2) experiments, excluding from optimization procedure pions as the lightest particles, the later circumstance can result in serious corrections, besides of Bose-Einstein enhancement effect in the distribution function, which we will discuss below. Then we describe the data in the model of a chemically equilibrated ideal hadron gas (HG). The feeding in our calculations is tuned according to the experimental conditions as described below.

In the geometry of the WA97 experiment the feed-down from weak cascade decays is expected to be of minor importance [23], and so the Λ ($\bar{\Lambda}$) have not been corrected for feed-down from Ξ weak decays, and Ξ have not been corrected for feed-down from Ω . But feeding of Λ ($\bar{\Lambda}$) from electromagnetic decays of Σ^0 ($\bar{\Sigma}^0$) is included. We did not include (according to the NA49 experimental procedure [8]) feeding of p and \bar{p} from $\bar{\Lambda}$, Λ and from Σ^+ , $\bar{\Sigma}^+$. In the NA49 experiment Λ and $\bar{\Lambda}$ yields include the contributions of Σ^0 and $\bar{\Sigma}^0$ as well as feed-down from weak Ξ decays [8]. The feeding of π^- from kaons and from Λ is not included [7]. We included feeding from ϕ decay into kaons (NA49 and WA97) and pions (NA49). For technical reasons in the model calculations we used the following substitution: $K_s^0/\pi^- \rightarrow (K^- + K^+)/2\pi^-$, a good approximation for Pb+Pb collisions [24]. The results for the best fit are shown in Tables 1 and 2 for Boltzmann statistic (BS) and quantum statistic (QS) calculations. The obtained temperatures $T_{ch} \approx 164$ MeV and baryochemical potential $\mu_B \approx 224$ MeV differ slightly from the corresponding values of Ref. [2], $T_{ch} \approx 168$ MeV, $\mu_B \approx 266$ MeV, that were gotten from analysis of particle number ratios in different limited rapidity intervals as well as in full 4π -geometry.

TABLE 1. Experimental particle number ratios (WA97) in Pb+Pb SPS collisions, compared to model calculation for Boltzmann statistic (BS) and quantum statistic (QS)

T_{ch}		163.37 MeV	163.91 MeV
μ_B		223.6 MeV	224.0 MeV
μ_S		55.2 MeV	55.1 MeV
Ratios	Data	BS	QS
$\Lambda/\bar{\Lambda}$	0.133 ± 0.007 [23]	0.133	0.133
Ξ^+/Ξ^-	0.249 ± 0.019 [23]	0.250	0.249
$\Xi^-/\bar{\Lambda}$	0.100 ± 0.004 [23]	0.098	0.099
$\Xi^+/\bar{\Lambda}$	0.188 ± 0.016 [23]	0.186	0.186
Ω^-/Ξ^-	0.182 ± 0.022 [23]	0.139	0.140
Ω^+/Ξ^+	0.281 ± 0.053 [23]	0.274	0.274
Ω^+/Ω^-	0.383 ± 0.081 [23]	0.492	0.489
Λ/K_s^0	0.6706 [25]	0.6212	0.6226

TABLE 2. Experimental particle number ratios (NA49) in Pb+Pb SPS collisions, compared to model calculation for Boltzmann statistic (BS) and quantum statistic (QS).

T_{ch}		163.37 MeV	163.91 MeV
μ_B		223.6 MeV	224.0 MeV
μ_S		55.2 MeV	55.1 MeV
Ratios	Data	BS	QS
$(p - \bar{p})/\pi^-$	0.184 [7]	0.245	0.239
$(p - \bar{p})/K^-$	1.776 [7,24]	1.847	1.843
$(p - \bar{p})/K^+$	1.028 [7,24]	1.090	1.086
K^+/K^-	1.727 [24]	1.695	1.697
\bar{p}/p	0.115 [7]	0.066	0.067
$\phi/(p - \bar{p})$	0.0802 [7,24,26]	0.0937	0.0935

The deviation between calculated particle ratios and experimental data are within the error of the data of WA97, excepts for the ratios which contain Ω . As to the \bar{p}/p ratio of NA49, one has take into account that the corresponding data $\bar{p}/p \approx 0.11$ are rather preliminary and differ much from published NA44 data where the value is twice less [27]. It is interesting to note, that in rapidity interval $2.0 < y < 2.5$ shifted by 0.65 units of rapidity from central mid-rapidity point, the correspondent value measured by NA49 [29] is 0.06 ± 0.01 .

As one can see from Table 2 the most significant deviation between model and data is for the $(p - \bar{p})/\pi^-$ ratio where the calculations predict a value about 30 percent larger then observed. Considering typical sizes of systematic errors in the data of at least 10 percent one should, however, not overestimate the statistical relevance of the discrepancy. In part, it maybe due to the reduction, compared to the results of Ref. [2], in μ_B since there are less baryons at mid-rapidity then are expected in scenario of full baryon stopping. Because about 1/2 of the pions result from baryonic resonance decays this also leads to a reduction of pions in the model and, thereby, over-prediction of the $(p - \bar{p})/\pi^-$ ratio.

The above effects of the non-uniformity in rapidity of the baryochemical potential can be estimated numerically. First, note that our result for $(p - \bar{p})/\pi^-$ ratio implies the same effective volume for pions as for other heavier hadrons. In fact, the pion volume is larger due to pion contribution from resonance decays. To explain that, let us, first, note that because of large resonance masses, comparing with the thermal freeze-out temperature, the momentum rapidity y of a resonance coincides with the rapidity η of the corresponding decaying fluid element and, therefore, the distribution of resonances in y follows their distribution in space-time rapidity η . The latter is determined mainly by the baryochemical potential that has a shallow minimum at $\eta = 0$. When resonances decay into the lightest particles, pions, there is a rather wide kinematic “window” Δy in rapidity for emitted pions. Then resonances with y beyond mid-rapidity may affect the multiplicities of pions at mid-rapidity. It is similar to a diffusion process: there is transport of pions from baryon rich peripheral y - regions to the central region. One can roughly estimate the effect of pion “diffusion” towards mid-rapidity using an effective temperature T_{dec} for those pions resulting from baryon decays. Taking into account that $m_\pi/T_{dec} \sim 1$, one can see from Eqs.(13) and (15) with substitution $ch \rightarrow th$, that a correction, increasing the effective volume for pions produced by baryonic resonances, could appear. Our numerical estimate is based on the baryonic density profile for AGS energies taken from Ref. [6], gives a contribution of about 10 % for pion transport to mid-rapidity region. Whether there are other mechanisms increasing, in particular, the number of pions at mid-rapidity, such as decay of a potentially formed disoriented chiral condensate, cannot be decided by the present analysis.

To provide the hydrodynamic calculations and estimate the energy density one may, phenomenologically, “fix” $(p - \bar{p})/\pi^-$ ratio by introducing an additional chemical potential for direct pions at chemical freeze-out of $\mu_\pi = 89$ MeV. Note, however, that the apparent anomaly in $(p - \bar{p})/\pi^-$ ratio has only little influence on the hydrodynamic behavior of chemically frozen HG considered in the next section.

IV. HYDRODYNAMIC EVOLUTION OF CHEMICALLY FROZEN HG

We describe hadron matter evolution at mid-rapidity after hadronization by the relativistic hydrodynamics equations for an ideal fluid:

$$\partial_\mu T^{\mu\nu} = 0, \quad \partial_\mu u^\mu n_i = 0, \quad (16)$$

where $T^{\mu\nu} = (\varepsilon + p)u^\mu u^\nu - g^{\mu\nu}p$ is the energy-momentum tensor of the Boltzmann-like gas (see Sec. II), $\varepsilon = \sum \varepsilon_i$ is energy density and $p = \sum p_i$ is pressure. We assume a quasi-inertial, Bjorken-like, longitudinal flow with velocity

$v = z/t$ at the post-hadronization stage of evolution. Thereby 4-velocities are described by Eq. (7). The energy densities are proportional to the profile factor $\rho(x)$ similar to density of particle species "i" (2): $\varepsilon_i(x) = \rho(x)\bar{\varepsilon}_i(x)$. Here $\bar{\varepsilon}_i(x)$ are thermodynamic energy densities in the Boltzmann gas. The equation of state for such a system has the form:

$$p = nT, \quad n = \sum n_i. \quad (17)$$

Due to chemical freeze-out the conservation of particle number density currents for each species of hadrons is explicitly implemented in Eqs. (16). We ignore the possible change of the particle number concentration during the relatively short hadronic expansion, since even for most intensive inelastic reactions such as resonance decays and baryon-antibaryon annihilation the role of back reactions is rather essential, as was discussed in Ref. [28].

Assuming that the hypersurfaces $\sigma(x)$, where the flow is in a quasi-inertial regime (7), correspond to the proper time $\tau(r, \eta) = \sqrt{t^2 - z^2} \approx const$ and using the non-relativistic approximation for transverse flow $v_T \equiv v$ (in LCMS):

$$v^2 \ll 1, \quad v \ll \frac{r}{\tau}, \quad \frac{\partial v}{\partial r} \ll \frac{1}{\tau} \quad (18)$$

one can get from Eq. (16), in a way similar to Ref. [30], the approximate hydrodynamic equations

$$\frac{\partial \varepsilon}{\partial \tau} + \frac{(\varepsilon + p)}{\tau} = 0, \quad (19)$$

$$(\varepsilon + p) \frac{\partial v}{\partial \tau} + \left(\frac{\partial}{\partial r} + v \frac{\partial}{\partial \tau} \right) p = 0, \quad (20)$$

$$\frac{\partial n_i}{\partial \tau} + \frac{n_i}{\tau} = 0, \quad (21)$$

and the exact equation

$$\frac{1}{\tau} \frac{\partial}{\partial \eta} p = 0. \quad (22)$$

Note that the equations (19)-(22) are related, in general, to non-uniformly distributed energy and particle densities. Among them, the last equation (22) is the only one that governs the dependence of densities on fluid rapidity η . The others contain η as a parameter. It allows us to analyze the solutions of the hydrodynamic equations (19)-(21) for any fixed rapidity. Our special interest concerns the point $\eta \approx 0$ corresponding to the main contribution to multiplicities at central rapidity.

Using the equation of state (17) and conservation of particle number density currents (21), one can rewrite Eqs. (19),(20) in the form:

$$C_V(T) \frac{\partial T}{\partial \tau} + \frac{T}{\tau} = 0, \quad (23)$$

$$\frac{\partial}{\partial \tau} (v\tau\omega) = -\tau \frac{\partial p}{\partial r}, \quad (24)$$

where

$$C_V(T) = \frac{\partial e(T)}{\partial T}, \quad e(T) = \sum \kappa_i e_i(T), \quad \kappa_i \equiv \frac{n_i}{n} = \frac{\bar{n}_i^{ch}}{\bar{n}^{ch}}, \quad e_i(T) \equiv \frac{\varepsilon_i}{n_i} = m_i \frac{K_1(m_i/T)}{K_2(m_i/T)} + 3T. \quad (25)$$

We will search for the solutions of Eqs. (23),(24) using a factorized ansatz for the profile factor: $\rho(x) = \rho_T(r)\rho_L(\eta)$ and assuming that it does not depend on τ . Then, from Eqs. (21), (24) and (25), we get the equation for the transverse velocity $v(r, \tau)$:

$$v(r, \tau) = v(r, \tau_{ch}) \frac{e(T_{ch}) + T_{ch}}{e(T) + T} - \frac{\partial \log \rho(r)/\partial r}{e(T) + T} \int_{\tau_{ch}}^{\tau} T(\tau') \partial \tau'. \quad (26)$$

The solutions (23), (26) of the hydrodynamic equations (19)-(21) can be found numerically by using, e.g., program package Mathematica [31]. First, from the Eq.(23) we find the temperature as the function of τ in the approximation of no transverse expansion, and after that calculate the transverse velocity from Eq.(26). Note that our solutions

correspond to hydrodynamic equations with non-constant velocity of sound $c_0^2(\varepsilon, n_i) = p/\varepsilon$. They describe non-relativistic transverse flows to first order. It is possible to find the second order terms, if one takes into account the next order terms for transverse flow in the all basic relativistic equations (16). To 2^{nd} order the profile factor ρ_T depends also on τ , e.g., if it has initially Gaussian form, it loses that form and becomes more flat (with sharp edges) when τ increases. However, the effective volume V_{eff} (11) does not change its value as compared with the first approximation and is still proportional to τ .

One can see that the equation for temperature (23) depends only on the concentrations κ_i of different particles species and does not depend on absolute values of densities, and, so, does not depend on the unknown common chemical potential μ_{ch} . The concentrations κ_i are completely defined by the temperature and baryochemical potential that are extracted from the fitting of particle number ratios (see Sec. III). Then Eq. (23) gives the possibility to find the proper time of chemical freeze-out τ_{ch} if one knows the initial conditions: temperature and proper time τ_{th} at thermal freeze-out. The latter values, as well as the transverse size and intensity of transverse flow at thermal freeze-out, can be found from analysis of p_T -spectra and HBT correlations. Then solving (23) numerically with condition $T(\tau_{th}) = T_{th}$ at thermal freeze-out, we find $T(\tau)$, and then find τ_{ch} from the equation $T(\tau_{ch}) = T_{ch}$. It gives the possibility to find the effective volume at chemical freeze-out, $V_{eff}^{ch} = (\tau_{ch}/\tau_{th})V_{eff}^{th}$. Further, using the absolute value of rapidity distribution for some particles, e.g., for pions, we can find the common chemical potential μ_{ch} - the factor that changes the energy and particle number densities as compared to chemically equilibrated ideal gas. Finally all densities at chemical freeze-out can be determined. Using the Eq. (26) one can also obtain the transverse velocity $v(r, \tau)$ at chemical freeze-out for given profile $\rho_T(r)$.

V. RECONSTRUCTION OF THERMAL FREEZE-OUT STAGE

To reconstruct the thermal freeze-out conditions, we assume that the freeze-out happens in a rather narrow time interval at approximately constant temperature T_{th} . It corresponds in our solution to some proper time $\tau_{th} \approx const$. We choose the transverse profile factor at thermal freeze-out in Gaussian form, $\rho_T(r) = \exp(-r^2/2R_T^2)$; as we noted before, in the basic approximation it does not depend on time during the hydrodynamic evolution. Then we have for the effective volume (11): $V_{eff} \approx 2\pi\tau R_T^2$ and, as follows from Eq.(26), $v(\tau, r) = v'(\tau, 0)r$ for $v^2(\tau, r) \ll 1$ if the velocity distribution at thermal freeze-out is linear in r for small enough r . To extract the temperature and transverse flows at thermal freeze-out we fit in our model the experimental spectral slopes for different particle species.

The transverse spectra for direct particles can be expressed through the Wigner function:

$$\frac{d^2N}{2\pi m_T dm_T dy} = \int d\sigma_\mu^{th}(x) p^\mu f\left(\frac{p_\mu u^\mu(x)}{T_{th}}, \frac{\mu_{i,th}}{T_{th}}\right) \rho(x), \quad (27)$$

At a region of small p_T the contribution from the decay of resonances has a peak that results in a significant change of the slope of transverse spectra. At large p_T , the relative contributions of a resonance decays are distributed much more uniformly in p_T , especially if transverse flow takes place, so the slopes of the spectra are approximately the same as for direct particles [32]. At very high energies $p_T > 2$ GeV particles from the hard partonic processes at the early collision stage may contribute to the spectra. We are fitting the transverse spectra according to Eq.(27) in the m_T -interval between 0.3 and 2 GeV/c for pions, kaons and protons. For hyperons we use an interval up to 3 GeV/c.

The other important point is how our results are influenced by the velocity profile. According to Eq. (26) the Gaussian form of density $\rho_T(r)$ dictates the linearity of the transverse velocity in r at small r if initial velocity profile is linear for small r . Of course, such an approximation is associated with the non-relativistic approach for transverse flow. Note that the integration in Eq.(27) is carried out over all r -region requiring to use correct velocity distributions when $v(r, \tau) < 1$ in the whole region $r < \infty$. So we have to extrapolate relativistically the velocity distribution in the r -region of applicability of our hydrodynamic solution, where $v^2(r, \tau) \ll 1$, to larger r . For this aim we use the results of Ref. [33] where two "extreme" relativistic extrapolations of a linear transverse velocity distribution from non-relativistic region to relativistic one was used:

$$v(r, \tau_{th}) = \tanh(rv'(\tau_{th}, 0)) \quad (28)$$

and

$$v(r, \tau_{th}) = rv'(\tau_{th}, 0)/\sqrt{1 + (rv'(\tau_{th}, 0))^2}, \quad (29)$$

where $v(r, \tau_{th}) \approx rv'(\tau_{th}, 0)$ for small transverse velocity $v(r, \tau_{th})$. The extrapolation (28) corresponds to "hard" flow, while the extrapolation (29) - to "soft" one [33]. We have used both of them to fit spectra and found that the deviation in extracted temperature T_{th} as well as in $v'(\tau_{th}, 0)$ is about 5 percent. It means also that for SPS energies the

relativistic tails of transverse velocity profile have no essential influence on the spectra in above mentioned momentum region, the transverse expansion, therefore, is basically non-relativistic. Thus we reproduce the plots of spectra for only one velocity profile corresponding to the "hard" flow, see also discussion in Ref. [33].

There are two fitting parameters in the analysis of the slopes of transverse spectra according to Eq.(27): T_{th} and $\alpha_{th} = (v'(\tau_{th})R_T)^{-2}$, where $1/\sqrt{\alpha}$ is the intensity of transverse flow [33], [13]

$$\sqrt{\alpha} = \frac{(v'_T(0))^{-1}}{\overline{R}_T} = \frac{\text{hydrodynamical length}}{\text{transverse radius}}. \quad (30)$$

One can see that $1/\sqrt{\alpha}$ is the hydrodynamic velocity at the Gaussian "boundary" of the system, $1/\sqrt{\alpha} = v(r = R_T)$, within a linear approximation for the velocity profile. For very intense relativistic transverse flow, $\alpha \rightarrow 0$. On the other hand for $\alpha \gg 1$ we have non-relativistic transverse flow. The results of the fit are presented at Fig. 1 and Fig. 2.

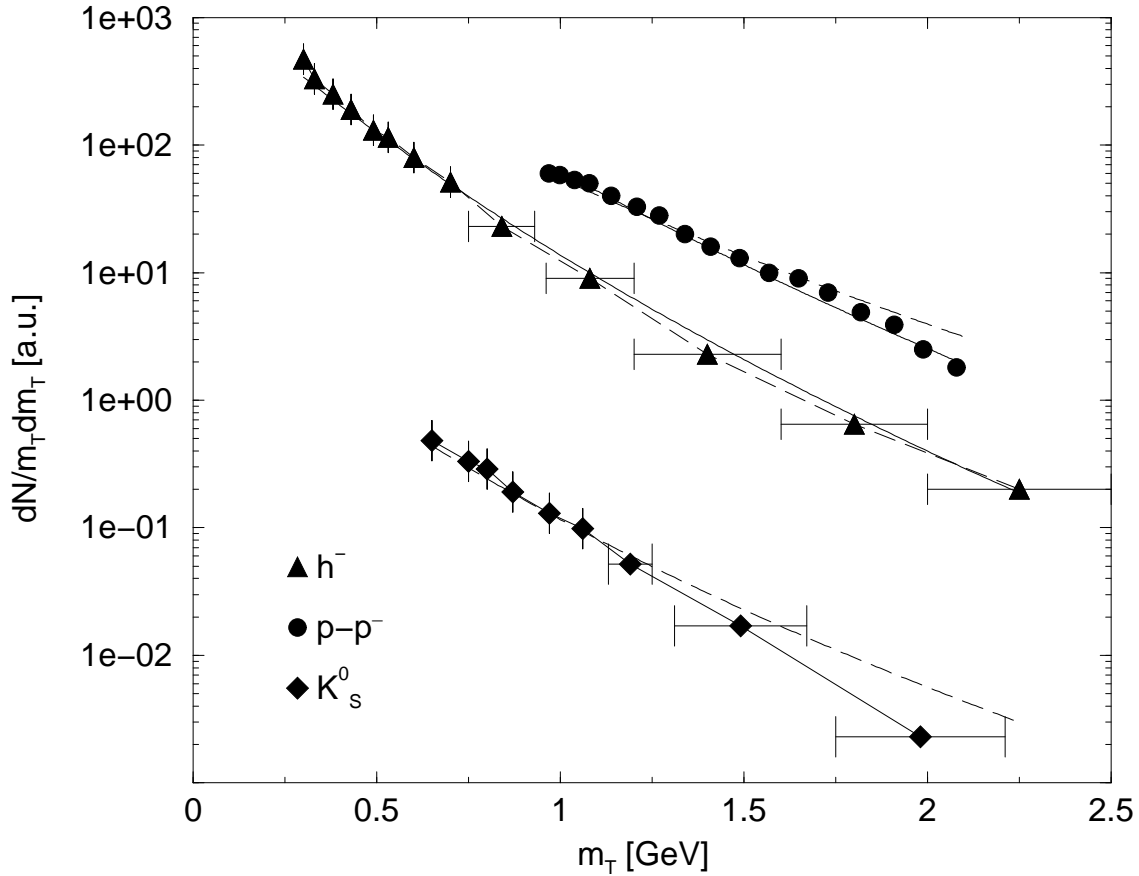


FIG. 1. The one-particle transverse mass spectrum for $p - \bar{p}$ [8], h^- and K_S^0 [34]. Solid line corresponds to $T_{th} = 135$ MeV and $\alpha_{th} = 7$, dashed line: $T_{th} = 100$ MeV and $\alpha_{th} = 4$. The overall normalization is arbitrary.

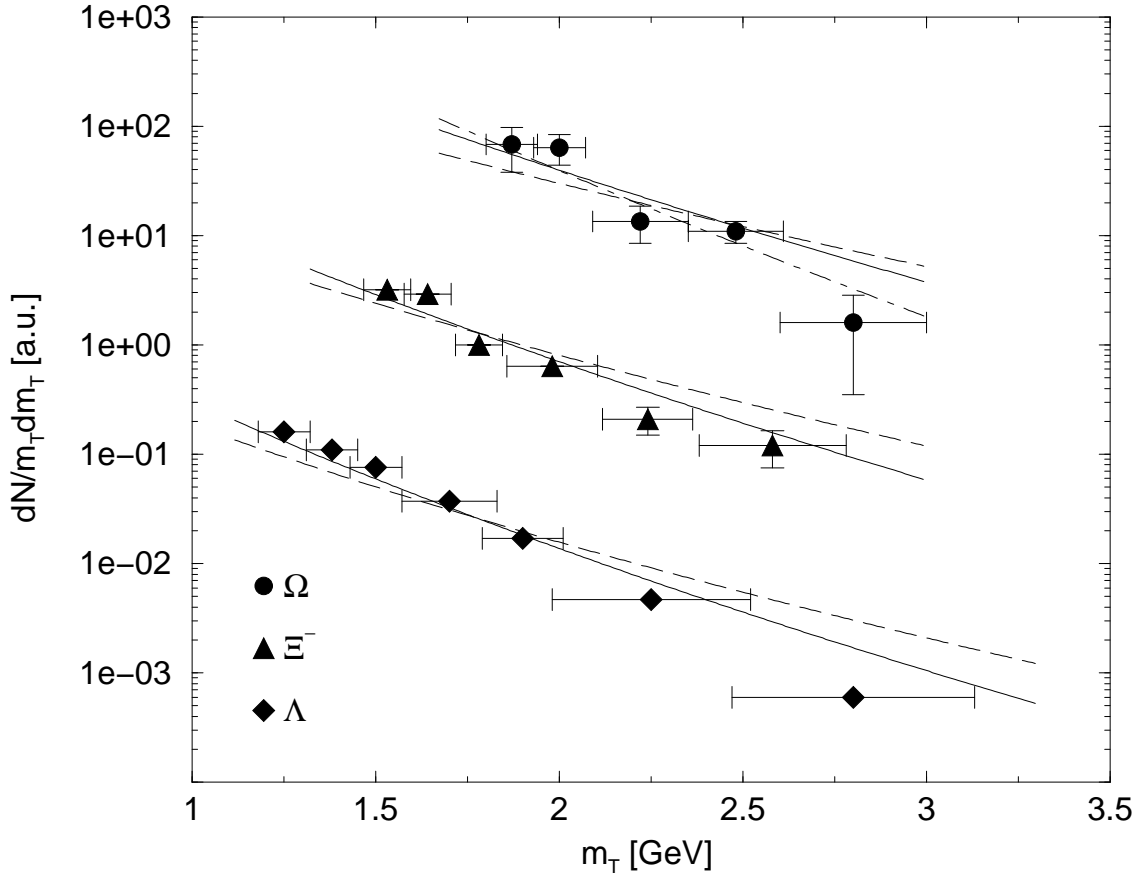


FIG. 2. The one-particle transverse mass spectrum for $\Omega = \Omega^- + \Omega^+$, Ξ^- and Λ [34]. Solid line: $T_{th} = 135$ MeV and $\alpha_{th} = 7$, dashed line: $T_{th} = 100$ MeV and $\alpha_{th} = 4$, dash-dotted line correspond to chemical freeze-out parameters: $T_{ch} = 163.37$ MeV and $\alpha_{ch} = 13.7$. The overall normalization is arbitrary.

As one can see from Fig. 1 the pion spectra can be described with good accuracy in two regimes: relatively low temperature of thermal freeze-out, $T_{th} = 100$ MeV and semi-relativistic transverse flow, $\alpha_{th} = 4$, on the one hand and higher temperature $T_{th} = 135$ MeV and non-relativistic transverse flow (within the typical size of the system at freeze-out R_T), $\alpha_{th} = 7$, on the other hand. While the latter parameterization describes well the spectra of all particles, except, possible, the baryon Ω , the former cannot reproduce the data on spectral slopes except for pions (see Figs. 1, 2).

It is worth to note that the transverse spectra for Ω could be described rather well, if one assumes that it escapes from the system just after hadronization with corresponding chemical freeze-out parameters: $T_{ch} \approx 163.37$ MeV and $\alpha_{ch} \approx 13.7$, the latter is evaluated from the hydrodynamic equations (see next section) with "initial" values $T_{th} = 135$ MeV and $\alpha_{th} = 7$ at thermal freeze-out. The satisfactory result for the Ω -transverse spectra with chemical freeze-out parameters, presented in Fig. 2, justifies the assumption of earlier freeze-out for Ω that could happen just after hadronization due to small cross-sections of these particles.

Finally we fix the thermal freeze-out parameters $T_{th} = 135$ MeV and $\alpha_{th} = 7$ according to the best fit for the set of transverse spectral slopes for pions, kaons, protons, Λ , Ξ and Ω . Another parameterization, which we demonstrate for comparison, $T_{th} = 100$ MeV and $\alpha_{th} = 4$, is closed to that in Refs. [14]. The reason to use such parameterization was that relatively large transverse flow corresponding to $\alpha_{th} = 4$ gives the possibility to describe satisfactorily the decrease of the observed pion interferometry radii with increasing of p_T . As a consequence, the temperature of thermal freeze-out becomes low, about 100 MeV. Such interplay between flow and temperature is easy to understand qualitatively from a simple approximation for spectral slopes:

$$T_{i,eff} \approx T_{th} + m_i/\alpha_{th}, \quad (31)$$

that is valid for heavy mass particles and non-relativistic flow [13]. As one can see from Fig. 1 and Fig. 2, such a low temperature parameterization fails to reproduce the spectra slopes for p , K , Λ , Ξ and Ω particles.

To discuss the problem, we would like to draw attention to resonance decay as an important factor that could influence the behaviour of the interferometry radii in p_T , a factor that was not yet taken into account quantitatively.

It is rather difficult because one needs to take into account of a large number of resonances. We note that the wide spread opinion that due to relatively small temperatures in hadron resonans gas one can use only resonances with low masses is not quite correct and, at least, needs verification, because the number of resonance states at a fixed mass interval increase quickly with mass.

Generally, the contribution of resonance decays into the final particle correlation function is a rather complicated effect. Namely, the resulting resonance contribution to the interferometry radii depends mostly on the following: statistical weight and mass distribution of resonances in the rest frame of fluid element, the intensity of flow, lifetime of resonance, feeding from middle-lived resonances, such as ω , and the kinematic "window" for pions coming from resonance decay. The important factor is also the length of the region of homogeneity [35], that is effective size of fluid element emitting the resonance in some p_T region, for developed flows it is rather less than the corresponding values for pions due heavier resonance masses. All these factors vary for different resonances and we cannot *a priori* exclude or easily estimate the influence of resonance decays on the interferometry radii at CERN SPS A+A collisions. Qualitatively, the steep decrease of the observed interferometry radii on p_T could be due to an interplay between two factors: transverse expansion of the hydrodynamic tube and contribution to the radii from resonance decays. For relativistic transverse flow the contribution of low-mass resonance decays to the interferometry radii is negligible [36], [32] and the decrease is determined mostly by flow. If the transverse expansion is not very intensive, the decrease of the interferometry radii on p_T is the result of both effects: flow and decays of resonances [37]. Therefore, in our opinion, the detailed evaluation of the resonance contribution to interferometry radii in hydrodynamic approach needs a serious study, taking into account the contribution of high mass resonances. In this paper we analyze the interferometry radii for pions, kaons and protons at maximal measured p_T region only, in order to minimize the influence of resonance contribution.

Our calculation of Bose-Einstein and Fermi-Dirac correlation function,

$$C^{ij}(p, q) = p_1^0 p_2^0 \frac{d^6 N_{ij}}{d^3 \mathbf{p}_1 d^3 \mathbf{p}_2} / \left(p_1^0 \frac{d^3 N_i}{d^3 \mathbf{p}_1} p_2^0 \frac{d^3 N_j}{d^3 \mathbf{p}_2} \right), \quad (32)$$

is based on the distribution function $f(p_\mu u^\mu(r, \eta)/T_{th}(\eta), \mu_{i,th}(\eta)/T_{ch}(\eta))$ in Boltzmann approximation at the hyper-surface of thermal freeze-out. For $\pi^- \pi^-$ correlation function we have, e.g.,

$$C(p, q) = 1 + \lambda \frac{\left| \int d\sigma_\mu^{th}(x) p^\mu f\left(\frac{p_\mu u^\mu(x)}{T_{th}}, \frac{\mu_{i,th}}{T_{th}}\right) \rho(x) e^{iqx} \right|^2}{\left(\int d\sigma_\mu^{th}(x) p_1^\mu f\left(\frac{p_{1\mu} u^\mu(x)}{T_{th}}, \frac{\mu_{i,th}}{T_{th}}\right) \rho(x) \right) \left(\int d\sigma_\mu^{th}(x) p_2^\mu f\left(\frac{p_{2\mu} u^\mu(x)}{T_{th}}, \frac{\mu_{i,th}}{T_{th}}\right) \rho(x) \right)} \quad (33)$$

where $p = (p_1 + p_2)/2$, $q = p_1 - p_2$ and λ is phenomenological parameter describing the experimental suppression of the correlation function due to, e.g., contribution of long-lived resonances. We are fitting by χ^2 -method the correlation function with fixed parameters $T_{th} = 135$ MeV and $\alpha_{th} = 7$ to Gaussian approximation of experimental data: $C(p, q_i, 0, 0) = 1 + \lambda \exp[-q_i^2 R_i^2(p)]$ in Bertsch-Pratt parameterization. Then $i = l, s, o$ correspond to longitudinal (l) and two transverse (t): sideward (s) and outward (o) directions.

Our results for proper time τ_{th} and geometrical Gaussian radius R_T of thermal freeze-out are presented in Table 3 in the last two columns. The experimental interferometry radii R_l and R_s for pion, kaon and proton pairs measured in LCMS near mid-rapidity are taken at maximum possible p_T . We assume, in agreement with experimental data for pion distribution in rapidity, that the longitudinal factor $\rho_L(\eta)$ does not vary strongly within one unit of rapidity near $\eta = 0$

TABLE 3. The characteristics of the thermal freeze-out in Pb+Pb SPS collisions. ²

	p_T GeV	R_l fm	R_s fm	R_T fm	τ_{th} fm
$\pi^- \pi^-$ [38]	0.5	4.6	4.25	5.3	8.2
$K^+ K^+$ [39]	0.91	3.2	3.59	5.1	8.9
pp [40]	1.073	2.9	3.4	5.2	9.5

Let us note that the proper time of thermal freeze-out τ_{th} and transverse radius R_T of system is slightly different for different pair correlation functions. To reconstruct the chemical freeze-out we will use the average values of the above parameters. In the Table 4 we compare our results (1st fit) with the results of other authors. Temperature,

²Two-dimensional fits for kaon and proton correlation functions in [39] and [40] were used.

proper time and transverse Gaussian radius of the system at thermal freeze-out for fits 2 – 4 are taken from Refs. [14], and for fit 5 from Ref. [15]. In the columns 4, 5 we present our results for the values of chemical potential of direct pions $\mu_{\pi,th}$ and average particle number density (before resonance decay) n_{th} at the thermal freeze-out, which were calculated by the method described in the next section for different parameters T_{th} , τ_{th} , R_T (fits 1 – 5).

TABLE 4. The characteristics of the thermal freeze-out in Pb+Pb SPS collisions.

Fit	T_{th} MeV	τ_{th} fm	R_T fm	$\mu_{\pi,th}$ MeV	n_{th} 1/fm ³
1	135	8.9	5.2	74.3	0.274
2	100	7.8	6.5	128.5	0.199
3	120	6.6	5.9	119.7	0.286
4	160	5.5	5.6	50.0	0.381
5	139	5.9	7.1	32.9	0.221

Of special interest is the average transverse velocity, that depends on the equation of state during the thermalized matter evolution after collision. At central slice of hydrodynamic tube the mean transverse hydrodynamic velocity $\langle v \rangle \equiv \langle |\mathbf{v}_T(\eta = 0)| \rangle$ and mean square of transverse hydrodynamic velocity $\langle v^2 \rangle$ are defined as follows:

$$\langle v^n \rangle = \frac{\int \frac{d^3p}{p^0} \int \frac{d\sigma_\mu}{d\eta} p^\mu v(x) f(x, p)}{\int \frac{d^3p}{p^0} \int \frac{d\sigma_\mu}{d\eta} p^\mu f(x, p)} = \frac{\int \frac{d\sigma_\mu}{d\eta} u^\mu(x) \rho(x) v^n(x)}{\int \frac{d\sigma_\mu}{d\eta} u^\mu(x) \rho(x)}, \quad n = 1, 2. \quad (34)$$

In the first approximation in $1/\alpha$ expansion one can get for $\alpha \gg 1$.

$$\langle v \rangle \approx \sqrt{\frac{\pi}{2\alpha}}, \quad \langle v^2 \rangle \approx \frac{2}{\alpha} \quad (35)$$

This approximation corresponds to non-relativistic flow and is model-independent (the result does not depend on relativistic extrapolation of the velocity profile, see discussion above). Then, at thermal freeze-out ($\alpha_{th} = 7$) we get for the average transverse velocity of the central ($\eta = 0$) slice of the hydrodynamic tube: $\langle v \rangle_{th} \approx 0.47$. The velocity at the Gaussian "boundary" of the system $1/\sqrt{\alpha_{th}} \approx 0.38$ justifies the applicability of our approach: non-relativistic transverse expansion.

Note, that using (31), one can get for cylindrically symmetric expansion the expression for transverse spectral slopes

$$T_{i,eff} \approx T_{th} + \frac{1}{2} m_i \langle v_{th}^2 \rangle = T_{th} + \frac{2}{\pi} m_i \langle v_{th} \rangle^2. \quad (36)$$

Right-hand side in the first equality is approximately the ratio of average transverse energy of particles species "i" in central slice, $\langle \frac{dE_{i,T}}{d\eta} \rangle \approx \frac{dN_i}{d\eta} T_{th} + \frac{dN_i}{d\eta} m_i \langle v_{th}^2 \rangle / 2$ to total number of particles of such species in central slice, $\frac{dN_i}{d\eta}$, at thermal freeze-out.

VI. HYDRODYNAMIC RECONSTRUCTION OF CHEMICAL FREEZE-OUT STAGE

Based on the hydrodynamic solutions found in Sec. IV and "initial conditions" at thermal freeze-out considered in Sec. V, we can restore the space-time extension of hadronization stage and find the particle and energy densities. In Fig.3 we demonstrate the cooling down of HG as it depends on proper time τ for fit 1. The "initial condition" for the hydrodynamic solution is the temperature of thermal freeze-out $T_{th} = 135$ MeV at corresponding time $\tau_{th} = 8.9$ fm/c which were found from the spectra and correlations in the previous section.

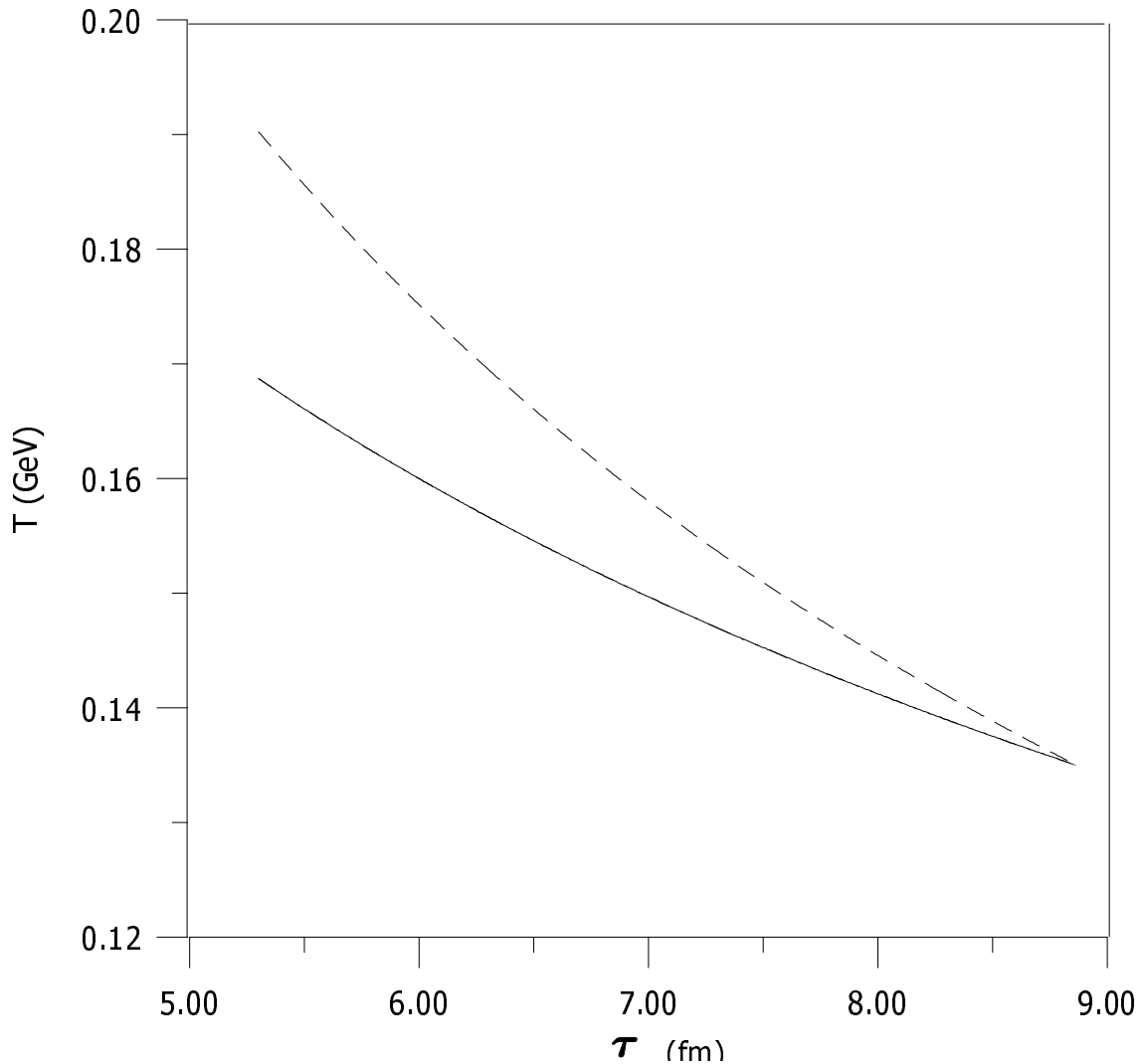


FIG. 3. The temperature T (GeV) of the hadron resonance gas as function of the proper time τ (fm/c) of its evolution. Dashed line describes limited case of the non-relativistic Boltzmann gas: $m_i \rightarrow \infty$. Solid line corresponds to the solution $T(\tau)$ of Eq.(23).

One can restore the proper time of the chemical freeze-out from the intercept of the curve $T(\tau)$ at the temperature of the chemical freeze-out $T_{ch} \approx 163.37$ MeV, that was found from the analysis of particle number ratios. Using the result, $\tau_{ch} = 5.7$ fm/c, one can calculate the effective volume $2\pi\tau_{ch}R_T^2 \approx 968$ fm³ associated to unit of rapidity at mid-rapidity, and then find common chemical potential μ_{ch} from pion multiplicities at mid-rapidity, $dN_{\pi^-}/dy \approx 160$ [7]. For direct pions the common chemical potential μ_{ch} is added to phenomenological one: $\mu_{\pi, ch} = \mu_{\pi} + \mu_{ch}$. Then one can easily evaluate the energy and particle densities.

Our results are presented in Table 5. The first line corresponds to parameters at thermal freeze-out which are represented in the first line of Table 4. In Table 5 we present also our results for proper time and densities at the hadronization stage based on the thermal freeze-out parameters taken from other papers: fits 2-5 from Table 4.

From the results presented in Table 5 one can see that the ratio of energy density to total particle density at chemical freeze-out reaches the value $\varepsilon_{ch}/n_{ch} = 0.997$ GeV, in agreement with the phenomenological observation in Ref. [41]. The similarity of these values in different relativistic nucleus-nucleus collisions could be an evidence that universal hadronization processes occur in all these reactions. The energy density at the hadronization point $\bar{\varepsilon}_{ch} \approx 0.42$ GeV/fm³ is close to results of lattice calculation at the region of the phase transition and about equal to the energy density inside a nucleon. Note that for temperature and chemical potential found in [2] at the chemical freeze-out, we get $\bar{\varepsilon}_{ch} \approx 0.54$ GeV/fm³ and $\varepsilon_{ch}/n_{ch} \approx 1.16$ GeV, that is close to our results. Using the values of concentrations of HG and temperatures at chemical and thermal freeze-out, we get for conventional velocity of sound $c_0^2 = p/\varepsilon = T/\sum \kappa_i e_i(T)$ the values 0.164 and 0.145 at chemical freeze-out and thermal freeze-out, respectively. Such relatively small values are determined by the large average mass of particles in hadron resonance gas, that is 0.662

GeV for hadronic masses below 2 GeV.

In Table 4 we list also the total particle number density \bar{n}_{th} , and chemical potential for direct pions $\mu_{\pi,th}$ at thermal freeze-out. One can see that for small temperature fits, $T_{th} = 100 \div 120$ MeV (fits 2 and 3) the chemical potential of direct pions at the stage of system decay seems to be too large and closed to condensation point, $\mu_{\pi,th} = m_{\pi}$.

From Eq. (26) and using the previously determined average velocity at the thermal freeze-out $\langle v \rangle_{th}$, we calculate the averaged velocity at chemical freeze-out $\langle v \rangle_{ch} \approx \sqrt{\frac{\pi}{2\alpha_{ch}}} = \sqrt{\frac{\pi}{2}} v'(\tau_{ch}, 0) R_T$ for fit 1. It is found that the average velocity at the hadronization is: $\langle v \rangle_{ch} \approx 0.339$ justifying the non-relativistic approximation *a posteriori*.

TABLE 5. The characteristics of the chemical freeze-out in Pb+Pb SPS collisions.

Fit	τ_{ch} fm	μ_{ch} MeV	$\bar{\epsilon}_{ch}$ GeV/fm ³	\bar{n}_{ch} 1/fm ³
1	5.7	-66	0.423	0.424
2	2.6	-9.0	0.600	0.602
3	3.3	-15.6	0.576	0.578
4	5.2	-75.9	0.398	0.399
5	4.1	-112.0	0.319	0.320

VII. CONCLUSIONS

The reconstruction of the hadronization stage for CERN SPS Pb+Pb collisions at 158A GeV/c is obtained within the hydrodynamic approach for the post-hadronization stage. Because of incomplete stopping at SPS energy we demonstrate that the analysis of particle ratios can be done within a relatively narrow rapidity window near mid-rapidity, provided one takes a non-uniformity in μ_B into account. We estimate that the non-uniformity of baryochemical potential may result in small but noticeable (≈ 10 %) contribution to the pion multiplicity at mid-rapidity due to transport of pions from resonance decays from non-central rapidity regions. Using an optimization procedure for the calculating particle number ratios near mid-rapidity, and also reconstructing the thermal freeze-out stage from spectra and correlations for different particle species, we find the physical conditions at the hadronization stage. The proper time for chemical freeze-out is found to be too small, $\tau_{ch} = 5.7$ fm/c to reach the chemical equilibrium in pure hadron gas, or cascade “event generator”, approach. The energy density is found to be close to the results of lattice calculations at the point of the phase transition. The ratio of energy density to total particle number density is found to be about 1 GeV that, seems, is the universal value for hadronization process.

ACKNOWLEDGMENTS

This work was supported by German-Ukrainian Grant No. 2M/141-2000, Ukrainian - Hungarian Grant No. 2M/125-99 and French-Ukrainian CNRS Grant No. Project 8917.

-
- [1] P.Braun-Munzinger, J.Stachel, J.P.Wessels, N.Xu, Phys. Lett. B **344**, 43 (1995); Phys. Lett. B **365**, 1 (1996).
 - [2] P.Braun-Munzinger, I.Heppe, J.Stachel, Phys. Lett. B **465**, 15 (1999).
 - [3] P.Koch, B.Muller, J.Rafelski, Phys. Rep. **142**, 167 (1986); H.Bebie, P.Gerber, J.L.Goity, H.Leutwyler, Nucl. Phys. B **378**, 95 (1992); J.Rafelski, J.Letessier, A.Tounsi, Acta Phys. Pol. B **27**, 1037 (1996).
 - [4] Yu.M.Sinyukov, S.V.Akkelin, A.Yu.Tolstykh, Nukleonika **43**, 369 (1998).
 - [5] J.Barrette et al, E877 Collaboration, Nucl. Phys. A **610**, 153c (1996); L.Ahle et al, E866 Collaboration, Phys. Rev. C **57**, R466 (1998); B.B.Back et al, (E917 Collab.), Phys. Rev. Lett. **86**, 1970 (2001).
 - [6] F.Shengqin, L.Feng, L.Lianshou, Phys. Rev. C **63**, 014901 (2000)
 - [7] F.Sikler for the NA49 Collaboration, Nucl. Phys. A **661**, 45c (1999).
 - [8] H.Appelshauser et al., (NA49 Collab.), Phys. Rev. Lett. **82**, 2471 (1999).
 - [9] A.Kostyuk, M.Gorenstein, H.Stocker, W.Greiner, Phys. Rev. C **63**, 044901 (2001).
 - [10] J.D.Walecka, Ann. Phys. **83**, 491 (1974); Phys. Lett. B **59**, 109 (1975); G.F.Bertch, S.Das Gupta, Phys. Rep. **160**, 189 (1988).
 - [11] J.Zimanyi, T.S.Biro, T. Csörgő, P.Levai, Phys. Lett. B **472**, 243 (2000).

- [12] C.M.Hung, E.Shuryak, Phys. Rev. C **57**, 1891 (1998).
- [13] Yu.M.Sinyukov, S.V.Akkelin, Nu Xu, Phys. Rev. C **59**, 3437 (1999).
- [14] B.Tomasik, U.A.Wiedemann, U.Heinz, nucl-th/9907096; U.A.Wiedemann, Nucl. Phys. A **661**, 65c (1999).
- [15] A.Ster, T. Csörgő, B.Lörstad, Nucl. Phys. A **661**, 419c (1999).
- [16] P.Braun-Munzinger, D.Magestro, K.Redlich, J.Stachel, hep-ph/0105229, Phys. Lett. B (in print).
- [17] P.Braun-Munzinger, J.Stachel, Nucl. Phys. A **606**, 320 (1996).
- [18] R.Stock, Phys. Lett. B **456**, 277 (1999).
- [19] J.Sollfrank, Eur. Phys. J. C **9**, 159 (1999).
- [20] L.D.Landau, Izv. Akad. Nauk SSSR, Ser. Fiz. **17**, 51 (1953).
- [21] J.D.Bjorken, Phys. Rev. D **27**, 140 (1983).
- [22] S. V. Akkelin, T. Csörgő, B. Lukács, Yu. M. Sinyukov and M. Weiner, Phys. Lett. B **505**, 64 (2001).
- [23] R.Caliandro for the WA97 Collaboration, J. Phys. G: Nucl. Part. Phys. **25**, 171 (1999).
- [24] C.Höhne for the NA49 Collaboration, Nucl. Phys. A **661**, 485c (1999).
- [25] L.Sandor for the WA97 Collaboration, talk at XXX International Symposium on Multiparticle Dynamics (ISMD 2000), Tihany, Hungary, 9-15 October 2000.
- [26] F.Sikler for the NA49 Collaboration, talk at XXX International Symposium on Multiparticle Dynamics (ISMD 2000), Tihany, Hungary, 9-15 October 2000.
- [27] M.Kaneta for the NA44 Collaboration, Nucl. Phys. A **638**, 419c (1998).
- [28] R.Rapp, E.Shuryak, Phys. Rev. Lett. **86**, 2980 (2001).
- [29] S.V.Afanasiev *et al.*, (NA49 Collab.), Phys. Lett. B **486**, 22 (2000).
- [30] P.Milyutin, N.Nikolaev, Heavy Ion Phys. **8**, 333 (1998); V.Fortov, P.Milyutin, N.Nikolaev, JETP Lett. **68**, 191 (1998); hep-ph/9901268.
- [31] Stephen Wolfram, Mathematica Version 3.0, Wolfram Research, Inc. 1996.
- [32] U.A.Wiedemann, U.Heinz, Phys. Rev. C **56**, 3265 (1997).
- [33] S.V. Akkelin, Yu.M. Sinyukov, Phys. Letters B356 (1995) 525; Z.Phys.C72 (1996) 501; Yu.Sinyukov, S.Akkelin, A.Tolstykh, Nucl. Phys. A **610**, 278c (1996).
- [34] F. Antinori *et al.*, (WA97 Collab.), Eur. Phys. J. C **14**, 633 (2000).
- [35] A.N.Makhlin, Yu.M.Sinyukov, Z. Phys. C **39**, 69 (1988); Yu.M.Sinyukov, Nucl. Phys. A **498**, 151c (1989); Yu.M.Sinyukov, Nucl.Phys.A **566**, 589c (1994); in: Hot Hadronic Matter: Theory and Experiment, eds. J.Letessier *et al.*, (Plenum Publ. Corp., 1995), p. 309.
- [36] Yu.M.Sinyukov, talk at Int. Workshop "Particle interferometry in high energy heavy ion reactions", ECT, Trento, September 1996 (unpublished).
- [37] J.Bolz, U.Ornik, M.Pumer, B.R. Schlei, and R.M. Weiner, Phys. Lett. B **300**, 404 (1993); Phys. Rev. D **47**, 3860 (1993).
- [38] R.Ganz for the NA49 Collaboration, Nucl. Phys. A **661**, 448c (1999).
- [39] D.M.Reichholde for the NA44 Collaboration, Nucl. Phys. A **661**, 435c (1999).
- [40] L. Conin, Ph.D. thesis, Paris, Orsay, 2001. See also at <http://www.star.bnl.gov/~conin/these-all.ps.gz>
- [41] J.Cleymans, K.Redlich, Phys. Rev. Lett. **81**, 5284 (1998); Phys. Rev. C **60**, 054908 (1999).